Chiral Diamine−Silver(I)−Alkene Complexes: A Quantum Chemical and NMR Study

Elsa Kieken,[†] Olaf Wiest,[†] Paul Helquist,[†] Maria E. Cucciolito,[‡] Germana Flores,[‡] Aldo Vitagliano,*[,‡] and Per-Ola Norrby*[,§]

Department of Chemistry and Biochemistry, University of Notre Dame, Notre Dame, Indiana 46556-5670, Dipartimento di Chimica, Università di Napoli "Federico II", Complesso Universitario di M.S. Angelo, via Cintia, I-80126 Napoli, Italy, and Department of Chemistry, Technical University of Denmark, Building 201, Kemitorvet, DK-2800 Kgs. Lyngby, Denmark

Received April 11, 2005

The ability of chiral diamine silver complexes to bind chiral and prochiral alkenes has been analyzed in detail. The stereoselectivity in binding of alkenes to a chiral ethanediamine silver complex has been investigated by NMR. The low-energy conformations of several small model complexes have been explored by DFT methods. By successive substitution of the computational model complexes, it has been possible to elucidate the role of each amine substituent in achieving successful discrimination of alkenes. The conformational space has been fully explored using small model systems, allowing an unbiased calculation of stereoselectivities that match well the experimental results. For a chiral allylic alcohol substrate, the correct stereoselectivity was obtained only when the structures were optimized with a continuum representation of the solvent. The discrepancy between gas phase and solution data is found to result from a competition between internal stabilization and solvation of the OH group of the substrate.

Introduction

Transition metal complexes are often used in bond-activation processes. Enantioselective coordination of transition metals to unsaturated compounds is of interest in asymmetric catalysis. It is also important in the field of chiral recognition and the resolution of racemic mixtures of unsaturated compounds. The enantioselective binding of one multiple bond is often achieved by means of chiral organic ligands bound to the metal center. The design of such chiral ligands for selective coordination of alkenes and alkynes can be very time-consuming by traditional trial-and-error methods. Since enantioselective binding of one enantiomer (or diastereomer) over its mirror image is based on the energy difference between the two complexes formed, this problem is particularly well suited for computational studies.

Silver cations form π-coordination complexes with alkenes.[1] Silver-based catalysts have been used in many useful reactions, some of which are alkene epoxidation,[2] amination of silyl enol ethers,[3] allylation of aldehydes,[4] and aziridination of alkenes.[5] As early as 1981, chiral silver complexes have been reported as NMR-shift reagents for the determination of enantiomeric purity of alkenes.[6] Recently, silver ions have been used as carriers for alkene transport through porous membranes.[7]

Some of us have recently been involved in studies of chiral ethanediamine ligands for enantioselective coordination of alkenes using copper(I)[8] as the metal center. These complexes can be used both as NMR-shift reagents and in the resolution of racemic alkenes. It was shown that a bulky substituent on each amine is vital to obtain good stereoselectivity. Other recent work by some of us has shown that similar silver complexes are also effective, both as NMR-shift reagents and as resolving agents for chiral alkenes.[9]

In the current work, we analyze the binding of chiral alkenes to silver in more detail, employing both experimental and theoretical methods. We began this work with two aims in mind: to rationalize the observed enantioselectivity and to gather data for development of rapid force field methods, which can be used in virtual screening of large numbers of potential ligands. The force field parametrization and virtual screening will be presented in later publications. In this paper, we focus on the details of the stereoselectivity in the binding of chiral alkenes to silver complexes of chiral diamine ligands.

* To whom correspondence should be addressed. E-mail: pon@kemi.dtu.dk.
[†] University of Notre Dame.
[‡] Università di Napoli "Federico II".
[§] Technical University of Denmark.

(1) Winstein, S.; Lucas, H. J. *J. Am. Chem. Soc.* **1938**, *60*, 836−847.
(2) For a leading reference to heterogeneous silver-catalyzed epoxidation, see: Linic, S.; Piao, H.; Adib, K.; Barteau, M. A. *Angew. Chem., Int. Ed.* **2004**, *43*, 2918−2921.
(3) (a) Yamashita, Y.; Ishitani, H.; Kobayashi, S. *Can. J. Chem.* **2000**, *78*, 666−672. (b) Kobayashi, S.; Yamashita, Y.; Ishitani, H. *Chem. Lett.* **1999**, 307−308.
(4) Shi, M.; Sui, W.-S. *Tetrahedron: Asymmetry* **2000**, *11*, 773−779.
(5) Cui, Y.; He, C. *J. Am. Chem. Soc.* **2003**, *125*, 16202−16203.
(6) Offermann, W.; Mannschreck, A. *Tetrahedron Lett.* **1981**, *22*, 3227−3228.
(7) (a) Chang, J. W.; Marrero, T. R.; Yasuda H. *J. Membr. Sci.* **2002**, *205*, 91−102. (b) Kim, J. H.; Min, B. R.; Won, J.; Kang, Y. S. *Chem. Eur. J.* **2002**, *8*, 650−654.
(8) Cavallo, L.; Cucciolito, M. E.; De Martino, A.; Giordano, F.; Orabona, I.; Vitagliano, A. *Chem. Eur. J.* **2000**, *6*, 1127−1139.
(9) Cucciolito, M. E.; Flores, G.; Vitagliano, A. *Organometallics* **2004**, *23*, 15−17.

10.1021/om050275t CCC: $30.25
Publication on Web 06/15/2005

Chart 1. Ligands Employed in the Computational Study

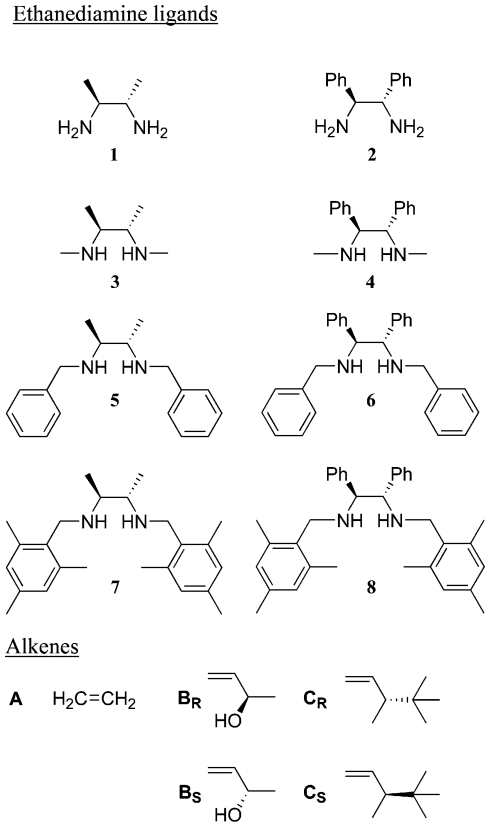

In the computational study, we have focused on the conformational preferences of the ligands, and in particular on the effect of different substituents on each type of conformational equilibrium, employing simplified model complexes for the conformational screening. The simplest possible complex of interest to us is composed of ethanediamine, silver cation, and ethene, with only one C_2-symmetric conformer (ignoring the enantiomeric conformer). To this complex we have

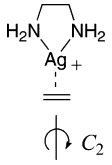

successively added backbone, nitrogen, and alkene substituents (Chart 1) and calculated the effect of each addition of substituents on selected conformational equilibria. With the DFT methods employed here, a full conformational search of the experimental systems is beyond our computational resources, but the successive increase of system size allows us to exclude groups of high-energy conformations using smaller model systems. The selection procedure allows us to find the most likely conformations of each isomeric complex and to compare the calculated data to the experimental results.

The NMR experiments have been focused on quantitatively determining the stereochemical preferences of the complexes with ligand **8**. The targets have been the configuration adopted by the nitrogen atoms upon coordination, the coordination modes of the chiral racemic alkenes **B** and **C**, and the relative binding affinities of the enantiomers of the chiral alkenes. Due to the high lability of the complexes, only partial information could be obtained about the first two targets, while an indirect method allowed an accurate determination of the last and most important point.

Methodology

In an extended study of silver−alkene cationic complexes, Schwarz and co-workers compared ab initio molecular orbital (MP2), density functional theory (LDA/BP), and density functional-Hartree−Fock hybrid methods (B3LYP).[10] All computational methods led to comparable results. The economical DFT hybrid methods are well suited to study these complexes and give results as accurate as more time demanding pure ab initio molecular orbital theory methods.

Another computational study of silver[2.2.2.]cyclophane π-prismands[11] at both the HF/3-21G* and B3LYP/3-21G* levels showed that results were in good agreement with available X-ray data, with a better accuracy for the DFT hybrid method. Furthermore, the study suggested that the counteranion to silver(I) can be omitted in the computational model. Finally, NBO analysis supported the σ-donation π-back-bonding coordination model for silver−alkene complexes.

DFT calculations on the cationic silver complexes, employing the B3LYP functional[12] together with the LACVP* basis set,[13] were performed using the Jaguar program.[14] Gas phase stationary points were confirmed by analytical calculation of frequencies. Energies for the solvated species were obtained by full optimization employing the PB-SCRF method[15] in Jaguar with parameters suitable for acetone (d^4_{20} = 0.7899, probe radius = 2.443 Å) and for chloroform (d^4_{20} = 1.4832, probe radius = 2.517 Å). All energies are reported in kJ/mol and are zero-point-corrected using the corresponding gas phase frequencies. Structures have been depicted using Molecule.[16]

Results and Discussion

The ligands and alkenes included in this study are shown in Chart 1. Each cationic ligand−silver−alkene complex is referred to by the ligand number and the alkene letter. Two types of backbone substituents have been considered: the small methyl (ligands **1**, **3**, **5**, and **7**) and the sterically more demanding phenyl (ligands **2**, **4**, **6**, and **8**). Both stereogenic carbons have the (*S*)-configuration in all ligands. In each series, the arms have been progressively elongated starting with primary amines (**1** and **2**) and moving to the smallest possible

(10) Hertwig, R. H.; Koch, W.; Schroder, D.; Schwarz, H.; Hrusak, J.; Schwerdtfeger, P. *J. Phys. Chem.* **1996**, *100*, 12253−12260.

(11) Saarenketo, P.; Suontamo, R.; Jodicke, T.; Rissanen, K. *Organometallics* **2000**, *19*, 2346−2353.

(12) (a) Becke, A. D. *J. Chem. Phys.* **1993**, *98*, 5648−5652. (b) Lee, C.; Yang, W.; Parr, R. G. *Phys. Rev. B* **1988**, *37*, 785−789.

(13) LACVP* uses the 6-31G* basis set for all light elements, and the Hay-Wadt ECP and basis set for Ag: Hay, P. J.; Wadt, W. R. *J. Chem. Phys.* **1985**, *82*, 299−310.

(14) *Jaguar 4.2*; Schrodinger, Inc.: Portland, OR, 2000. For the most recent version, see: http://www.schrodinger.com.

(15) Marten, B.; Kim, K.; Cortis, C.; Friesner, R. A.; Murphy, R. B.; Ringnalda, M. N.; Sitkoff, D.; Honig, B. *J. Phys. Chem.* **1996**, *100*, 11775−11788.

(16) *Molecule* for Macintosh version 1.3.5d9; http://www.ccc.uni-erlangen.de/molecule/

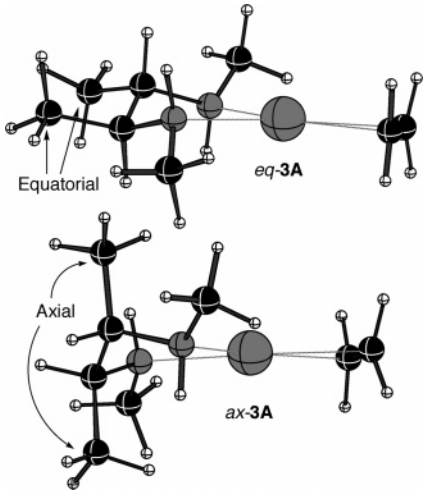

Figure 1. Selected isomers of **3A**.

secondary amine with methyl substituents (**3** and **4**). The bulkiness of the arms is then increased by addition of aryl substituents to yield first benzyl- (**5** and **6**) and finally mesityl-methyl-substituted ligands (**7**, **8**). The largest calculated ligand, **8**, is identical to that employed in the experimental studies.[9] We have first investigated each ligand complexed to silver and ethene (alkene **A**, Chart 1). Subsequently, the enantioselective recognition of chiral alkenes was studied by calculating the energy difference between the diastereomeric complexes formed upon coordination of silver to chiral alkenes. Two chiral alkenes were investigated: one allylic alcohol (alkene **B**) and one hydrocarbon (alkene **C**). Experimental results for complexes **8B** and **8C** have been reported earlier,[9] but a more detailed NMR analysis has been performed in the current work.

The ligand models are all chiral and C_2-symmetric. The backbone substituents can adopt either axial or equatorial positions by flipping the chelate ring. The secondary nitrogens become chiral upon coordination of the silver cation and can adopt either (*R*)- or (*S*)-configurations, putting the nitrogen substituents either *trans* or *cis* to the backbone substituents. The lability of the metal−nitrogen bond allows the substituent to find the thermodynamically most favored configuration in each complex.[8] Finally, the coordination of a chiral alkene adds facial diastereoselectivity, leading to 24 possible structures for each ligand−silver−alkene combination.

Due to the long N−Ag bonds (2.3−2.4 Å), the five-membered chelate ring is conformationally similar to a cyclohexane ring. In all calculated complexes, the backbone dihedral angle (N−C−C−N) adopts values close to ±60° (*gauche*). Complexes **1A**−**4A** have been minimized in the two possible chair-like conformations, with the backbone substituents in axial or equatorial positions (Figure 1).

Table 1 shows the energy difference between axial and equatorial conformers. For the ligands containing a secondary amine (ligands **3** and **4**), several configurations at N are possible (vide infra). Only the lowest energy conformers for each case (axial and equatorial backbone substituents) are compared in this section.

With primary amines (complexes **1A** and **2A**), the preference for equatorial over axial backbone substitution is small (1.6 and 0.6 kJ/mol, respectively) and falls within the error limits of the computational method. For complexes **3A** and **4A**, the lowest energy conformation obtained has all substituents in equatorial positions and thus *trans* to each other (e.g., *eq*-**3A**, Figure 1). The preference for the all-equatorial complex increases to 5−6 kJ/mol in the secondary amines. We therefore expect that the ligands with bulkier nitrogen substituents (ligands **5**−**8**) will have a strong preference for the all-equatorial conformation.[8,9] Thus, one important role of the nitrogen substituents is to lock the backbone conformation. In the rest of this work, only the complexes with secondary amines (ligands **3**−**8**) have been investigated, and the backbone substituents have been kept in equatorial position.

Table 1. Excess Energy of Axial vs Equatorial Backbone Substituents

complex	$E_{ax} - E_{eq}$ (kJ/mol)
1A	1.6
2A	0.6
3A	4.7
4A	6.3

Table 2. Relative Energies (kJ/mol) for Different Ligand Nitrogen Configurations

complex	(*R,R*)	(*R,S*)	(*S,S*)
3A	0.0	4.1	10.8
4A	0.0	11.4	21.3
5A	0.0	−1.9	3.8
6A	0.0	7.6	16.7
7A	0.0	5.3	6.5
8A	0.0	13.6	18.2

Upon coordination to the silver cation, the secondary amines become chiral. The nitrogen configuration is (*R*) when the substituent is *trans* to the backbone substituent. Three distinct ligand−silver complexes can be formed with respect to the chirality at N: (*R,R*), (*R,S*)—which is equivalent to (*S,R*)—and (*S,S*). The calculated relative energies for all configurations are shown in Table 2.

For ligands **5**−**8** with aromatic arms, a chiral pocket is formed that embraces the alkene, allowing favorable C−H···π interactions but requiring the alkene to twist (Figure 2). We see from the results in Table 2 that the (*R,R*) complex is favored in most cases. The only exception is complex **5A**, which can obtain two favorable C−H···π interactions between phenyl π-faces and alkene C−H bonds without requiring the alkene to twist, by switching one benzyl to an axial position (Figure 3). However, introduction of either backbone phenyl substituents (**6A**) or *ortho*-methyl groups on the phenyl rings (**7A**) disfavors the axial position of the nitrogen substituents, and for the largest complex, **8A**, we see a very strong preference for the (*R,R*)-configuration, where all substituents can occupy equatorial positions. The mesityl groups have an important role in limiting the configurational space of the ligand upon coordination to silver. Only the (*R,R*)-nitrogen configuration is considered henceforth.

The largest ethanediamine ligands (**5**−**8**) have two degrees of freedom per arm. The N−C bond can adopt one *anti* and two *gauche* conformations. The lowest

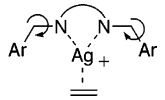

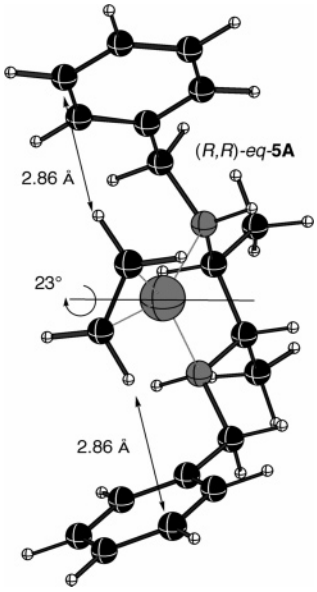

Figure 2. All-equatorial complex, showing twisting of alkene and favorable C−H···π interactions

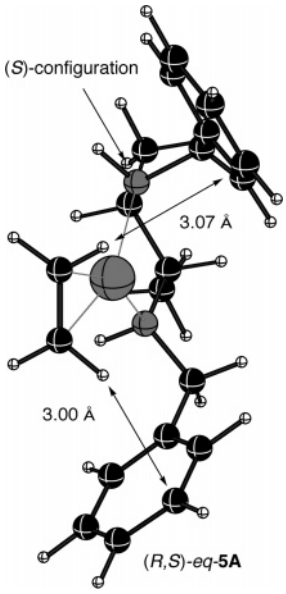

Figure 3. Unusual, favored (*R,S*)-configuration of **5A**.

energy conformation is obtained when both arms are in *anti* positions with respect to the ligand backbone. The energetic cost of putting one arm in a *gauche* position is at least 7 kJ/mol. The second degree of freedom of the arm is the aromatic ring rotation. The favored position of the aryl group is similar for both the phenyl and the mesityl rings, with a C−C−C−N dihedral angle of around 65°. However they differ highly in

terms of barrier of rotation: coarse scans with a resolution of 30° indicate barriers of around 10 and 34 kJ/mol for the phenyl and mesityl groups, respectively. The preferred conformation of the ligand upon coordination to silver, shown in Figure 4, forms a C_2-symmetric pocket in which the alkene can bind, flanked by aromatic units that can provide selective steric hindrance,[8]

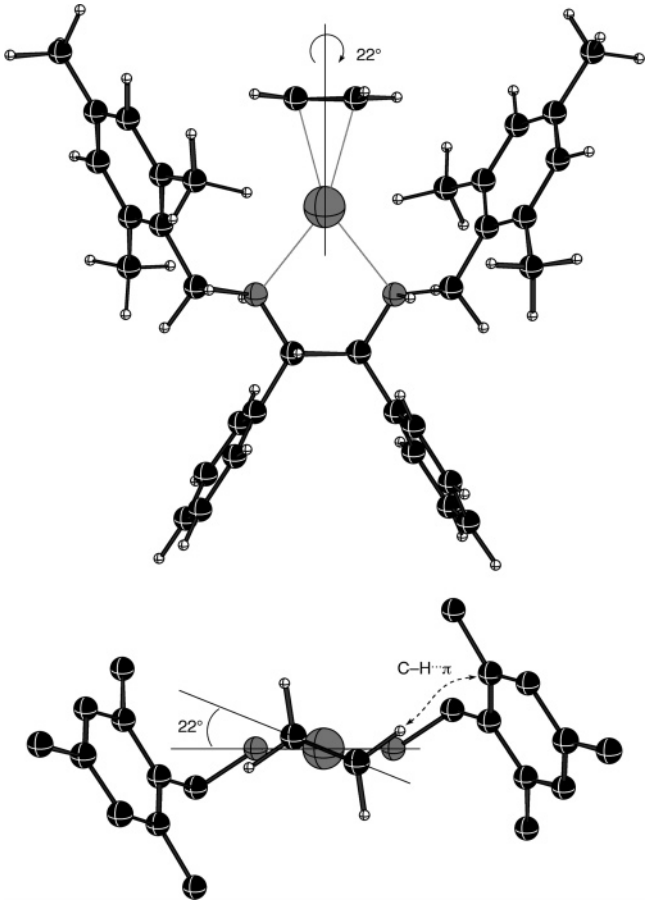

Figure 4. Complex **8A**.

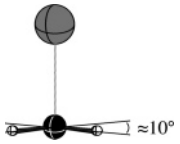

Figure 5. Dihedral angle as a measure of back-bonding.

but also stabilizing alkene C−H interactions with the π-system of the aromatic rings.

With unsymmetrical alkenes, additional factors such as face selectivity and position of the substituents on the alkene have to be considered. The alkenes coordinate with one π-orbital to the silver ion. Some back-bonding also occurs from a filled d-orbital of silver to the π^*-orbital of the alkene.[17] The back-bonding can be quantified by measuring a *trans*-H−C=C−H torsion or a *gem*-H−C(=C)−H improper torsion in the coordinated alkene of the computed structures. For ideally sp^2-hybridized alkenes the value is 180°, whereas complete sp^3-hybridization requires a value of 120°. The silver cation gives only moderate back-bonding; the DFT structures in the current work display torsions and improper torsions in the range 169−173° (Figure 5). We note that torsions including substituents larger than hydrogen sometimes display stronger deviations from planarity, due to repulsive interactions with the metal, and thus are less well suited for an unbiased evaluation of back-bonding.

The alkene clearly prefers to coordinate in the plane defined by silver and the two nitrogen ligands. In ethene

(17) (a) Dewar, M. S. *Bull. Soc. Chim. Fr.* **1951**, *18,* C71. (b) Chatt, J.; Duncanson. L. A. *J. Chem. Soc.* **1953**, 2939.

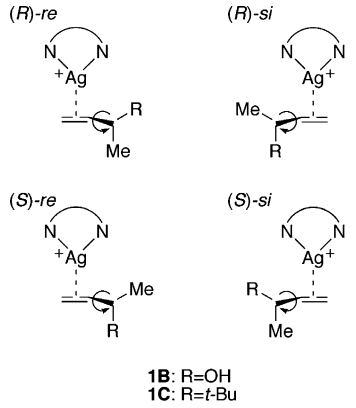

Figure 6. Conformational investigation of chiral alkene complexes **1B** and **1C**.

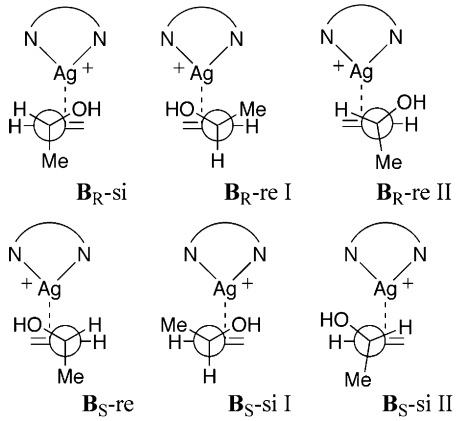

Figure 7. Low-energy isomers of coordinated alkene **B**.

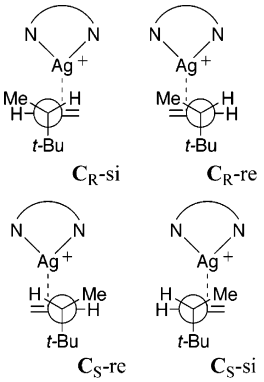

Figure 8. Low-energy isomers of coordinated alkene **C**.

complexes with the small ligands, **1A** through **4A**, the dihedral angle between the alkene−silver and nitrogen−silver planes is 0−2°. In the presence of aryl arms, the alkene rotates around the axis connecting its center to the silver atom. In the optimized geometries of **5A**−**8A**, the alkene rotates by more than 20° to allow two *trans* hydrogens on the alkene to form C−H···π interactions with the aromatic rings (cf. Figures 2 and 4; distances from hydrogen to the closest ring carbon <2.9 Å). With monosubstituted alkenes (**B** and **C**), only one pair of *trans* hydrogens is available to form the C−H···π interactions. Due to the offset of the aromatic rings from the coordination plane, the rotation required for binding differs for the *re*- and *si*-coordination modes, favoring *si*-coordination with the ligands employed herein (backbone (*S,S*)-configuration).

The chiral alkenes employed here (**B** and **C**) both have one methyl and one other substituent (hydroxyl or *tert*-butyl) in the allylic position. To investigate the available conformations in the silver complexes, we performed torsional scans around the allylic C−C bond with a resolution of 30°, for both *re*- and *si*-forms of complexes $\mathbf{1B}_R$, $\mathbf{1B}_S$, $\mathbf{1C}_R$, and $\mathbf{1C}_S$ (Figure 6), followed by full optimization of all low-energy rotamers identified in the scans. It is clear that there is a strong connection between the face selectivity, the chirality of the alkene, and the rotameric preference of the C−C bond.

In the allylic alcohol case (alkene **B**), coordination occurs between the silver cation and the oxygen for all low-energy conformers obtained (Figure 7). For all isomers, there exists a low-energy conformer where the oxygen is rotated close to the double bond (C=C−C−O torsional angle ca. 36°), but is still in contact with the silver. The methyl group clearly prefers an orientation orthogonal to the alkene plane, pointing away from the silver cation. For the $\mathbf{1B}_R$-si and $\mathbf{1B}_S$-re isomers, both of these criteria can be fulfilled simultaneously (Figure 7). Inverting the alkene chirality in these two isomers while keeping the face selectivity and oxygen orientation constant will give conformer **I** of complexes $\mathbf{1B}_R$-re and $\mathbf{1B}_S$-si. In this conformer, the allylic hydrogen is orthogonal to the alkene plane and the methyl group is pointing toward the position that will be occupied by the aromatic arms of the larger ligands **5**-**8**. Rotation around the allylic bond allows an alternative conformer, designated **II**, with the allylic C−H virtually eclipsed with the alkene double bond and the oxygen atom still coordinating to silver. The latter is predicted to be the preferred conformer for isomers $\mathbf{B}_R$-re and $\mathbf{B}_S$-si in complexes with ligands **5**−**8**. Calculations using a larger ligand (complexes **5B**) verify that conformer **I** is selectively disfavored by steric interactions with the benzylic arms. Thus, only conformers of type **II**, with the methyl group pointing away from and the oxygen coordinating to silver, will be considered. Other conformers could be generated for the various **1B** isomers, but all were found to be at least 6 kJ/mol higher in energy than the global minimum for each isomer.

For the alkenes **C**, due to the bulkiness of the *tert*-butyl group, the lowest energy rotamers are obtained with the *tert*-butyl group pointing away from the silver (Figure 8). Second minima were found with the *tert*-butyl group orthogonal to the alkene and pointing toward the silver. These rotamers are 5−7 kJ/mol higher in energy and will be selectively disfavored by nitrogen substituents. They will not be considered in the rest of this paper.

Keeping in mind the requirements previously mentioned, we can now investigate the enantioselectivity of the complexes containing the largest ligands. Backbone and nitrogen substituents are kept in equatorial positions, benzylic arms are positioned *anti* to the backbone forming a binding cleft, and the largest alkyl group on each alkene is oriented away from silver, but all four diastereomeric combinations were included. Complexes **5B**−**8B** and **5C**−**8C** were minimized. Relative energies are shown in Table 3.

Looking first at alkene **C**, we see a distinct preference for the (*R*)-*si* isomer, in particular with the largest

Table 3. Calculated Energy Penalty (kJ mol^{-1}) in Formation of Complexes with Chiral Alkenes

	R-si	*R-re*	*S-si*	*S-re*
5B	3.2	2.8[a]	0.0	5.7
6B	5.8	8.1	0.0	14.2[a]
7B	1.9	3.4	0.0	9.3
8B	6.7	9.2	0.0	11.8
5C	0.0	9.0	6.0	5.6
6C	0.0	9.9	5.3[a]	10.4
7C	0.0	11.9[a]	5.8	3.9
8C	0.0	13.1	5.8	12.8

[a] Vibrational analysis reveals one negative eigenvalue corresponding to a methyl rotation, with an imaginary frequency between −12 and −4 cm^{-1}. The structure does not improve on further optimization.

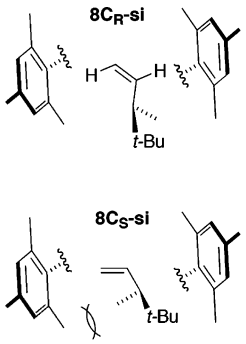

Figure 9. Pictorial representation of the most stable isomers of **8C**.

ligand, **8**. The rotation of the alkene in the **8C**$_R$-si complex is even more pronounced than in the ethylene complexes: the dihedral angle between the Ag−N−N and Ag−C═C planes is 37°. The two *trans*-hydrogens on the alkene form favorable interactions with the mesitylene rings, with shortest C−H···C contacts of ca. 2.96 Å on both sides and both the *tert*-butyl and methyl substituents positioned with almost ideal vdW contacts with one mesitylene moiety (Figure 9). In contrast, the other *si*-isomer, **8C**$_S$-si, shows very little alkene rotation. Both the higher energy and the lack of rotation can be traced to the position of the allylic methyl substituent, which is positioned very close to the alkene double bond and thus suffers from both allylic strain and steric repulsion from Ag. As shown in Figure 9, the alkyl groups are in vdW contact with one mesitylene each; any rotation of the alkene would lead to severe repulsion.

Both **8C**-re complexes suffer severe interactions between mesitylene and alkyl groups, leading to severe twisting. The dihedral angles between the ligand and alkene coordination planes are larger than 40°.

The allylic alcohol **B** shows some interesting features. Both **8B**-re complexes are distorted and disfavored, for the reasons already indicated (vide supra). However, for the *si*-complexes, we see that binding of the (*S*)-enantiomer is strongly favored, in clear contradiction with experimental data (vide infra). Upon closer inspection, we can see that the computational preference results from an O−H···π hydrogen bond in the **8B**$_S$-si isomer (Figure 10), with an O−H···C distance of 2.57 Å. In the corresponding **8B**$_R$-si complex, which should be favored in solution according to NMR, no such interaction is possible. This is an example of an electrostatic collapse, a known strong deficiency of gas phase

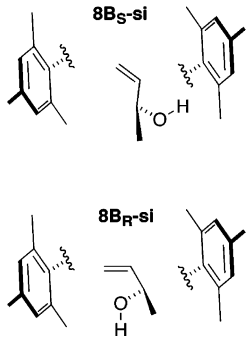

Figure 10. Hydrogen bonding causes inversion of population in gas phase calculations of **8B**.

Table 4. Re-evaluation of Diastereoselectivities Using a Continuum Solvation Model

		R-si	R-re	S-si	S-re
acetone	**8B**	0.0	11.0	1.5	14.8
	8C	0.0	15.2	8.5	9.0
chloroform	**8B**	0.9	12.4	0.0	14.0
	8C	0.0	33.3	22.8	26.9

calculations.[18] To overcome this difficulty, it is necessary to account for the effect of solvent. To this end, we have employed the PB-SCRF model,[15] which has previously shown good results for organometallic complexes.[19]

The four diastereomers of **8B** were reoptimized in solvent (acetone and chloroform). The results are shown in Table 4. We see that the solvation model decreases the difference between the two forms and in acetone even inverts the preference, so that we now reproduce the experimental selectivity. The remaining errors are in the range 2−4 kJ/mol, a very good result in view of the complexity of the problem.

NMR Studies

The possibility of experimentally investigating the solution stereochemistry of complexes **8** is bound to the rates of the various dynamic processes taking place in solution and interconverting the possible isomers. Most of these processes were expectedly found to be considerably faster for the Ag(I) species than for their Cu(I) analogues,[8] complicating and in some cases precluding an exhaustive determination of the abundances and configurations of the existing stereoisomers. We shall here examine the available NMR information and its stereochemical implications.

Complex 8A-BF$_4$. At room temperature (298 K) the ^{1}H NMR spectrum (CD_2Cl_2) shows individual multiplets both for the CH (δ = 4.33) and for the NH (δ = 3.31) protons of the diamine, while the diamine CH_2 protons appear as the AB part (δ = 3.55 and δ = 3.48) of a single ABX multiplet; the ethylene protons give a sharp singlet at δ = 4.21. This set of peaks indicates the presence of only one species in solution having C_2 symmetry (thus with the two N atoms displaying the same configuration), but it might as well be the result of a dynamic averaging of two or more species having different structures. Low-temperature experiments indicated that at room temperature there is indeed one largely domi-

(18) Boström, J.; Norrby, P.-O.; Liljefors, T. *J. Comput.-Aided Mol. Des.* **1998**, *12*, 383−396
(19) Norrby, P.-O.; Mader, M. M.; Vitale, M.; Prestat, G.; Poli, G. *Organometallics* **2003**, *22*, 1849−1855.

nant species (probably more than 95% abundance) rapidly interconverting with a very minor species, which becomes more abundant at low temperature. On lowering the temperature, the signals of the major species broaden (couplings disappear), and at 263 K, new small and broad signals appear. On further lowering the temperature, the main signals tend to become sharp again while the small signals considerably increase in area and also become sharper. At 233 K, the minor species (ca. 20% abundance) displays separate signals for each proton of the diamine skeleton, indicating loss of the C_2 symmetry. Notably, the two backbone CHPh protons of the minor species appear at $\delta = 4.98$ and $\delta = 4.34$ and display remarkably different couplings to the vicinal NH protons (5.5 and 12.3 Hz, respectively), a feature that can be considered diagnostic for a (*S, S, S, R*)-configuration of the diamine backbone.[8] A new, moderately broad signal also appears at $\delta = 5.14$ for the ethylene protons of the minor species, with an area consistent with the presence of two molecules of ethylene in the complex. It can therefore be concluded that **8A** in solution is an essentially pure trigonal C_2-symmetric species having the (*R, S, S, R*)-configuration, which is in equilibrium with a different species **8A′**, which appears to be a four-coordinate (most likely tetrahedral) complex containing two coordinated ethylene molecules and an (*S*, *S*, *S*, *R*) diamine backbone. For entropic reasons, this high molecularity species is disfavored at higher temperatures. In **8A**, the alkene protons are equivalent, despite the obvious pairwise nonequivalence in a C_2-symmetric complex, indicating rapid exchange between free and complexed alkene at all achievable temperatures.

Complex 8B-BF_4. In the room-temperature (298 K) ^{1}H NMR spectrum of the partially resolved diastereomer (ca. 85% abundance) containing the (*R*)-allylic alcohol (CD_2Cl_2), the signals of the diamine moiety display the same multiplicity as those of the ethylene complex **8A** described above. This indicates the presence of only one species in solution having C_2 symmetry (thus with the two N atoms displaying the same configuration and with the alkene in fast rotation around the Ag−double bond axis), but as stated above it might as well be the result of a dynamic averaging of two or more species having different structures. At lower temperature (228 K), small broad signals appear in the spectrum, which could not be specifically assigned, while the main signals, although slightly broadened, still indicate a predominant (>90%) C_2-symmetric species. Particularly relevant is the large upfield shift of the methyne C*H*OH proton ($\delta = 2.66$ versus $\delta = 4.20$ in the free alkene), which strongly suggests that this proton lies well within the shielding cone of the adjacent mesityl ring, thereby giving experimental support to the calculated most stable geometry of the complex (**8B**$_R$-si, Figure 10).

The enantioselectivity for the coordination of the (*R*)-allylic alcohol could in principle have been determined by adding some (*S*)-butenol to the sample and measuring the relative amounts of the two diastereomers and of the free alkene, as was done for the analogous Cu(I) complex.[8] However, in the presence of an excess of butenol, only very broad and partially coalesced signals could be obtained for the free and coordinated alkene even at temperatures down to 213 K, thus preventing a direct NMR determination of the enantioselectivity and forcing us to adopt the following alternative method.

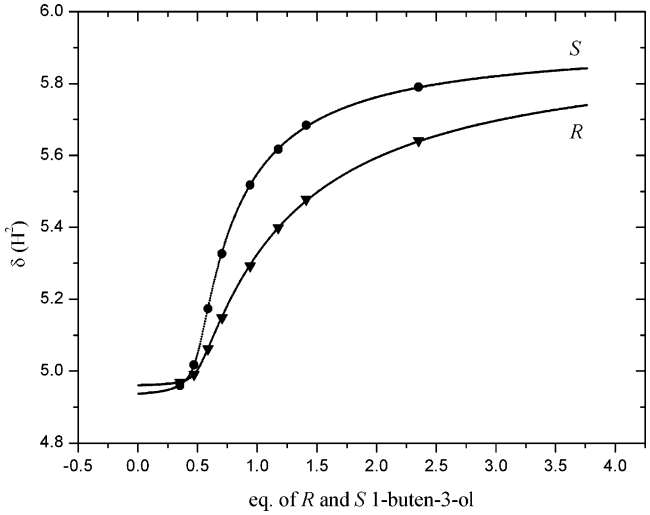

Figure 11. Calculated (lines) and observed (symbols) chemical shifts of the H^2 proton of 1-buten-3-ol as a function of the equivalents of each enantiomer added to the fragment [(*S,S*-8)Ag]OTf (12 mM in $CDCl_3$).

At room temperature, the exchange of free and coordinated alkene is fast on the NMR time scale, and the chemical shifts observed for each alkene enantiomer are the weighted averages of free and complexed forms. We performed NMR titrations, by adding increasing amounts of alkene racemate to a solution of [(N−N)-Ag]X. (N−N = **8**, X = triflate or nitrate). During the titration, the observed chemical shifts of the two alkene enantiomers move progressively toward the corresponding values of the free alkene, which are expected to be reached asymptotically when a large excess of alkene is added. The shapes of the resulting titration curves depend on the relative stabilities of the two diastereomers, the chemical shifts of the less stable one approaching more rapidly the common asymptotic value (see Figure 11 for an example). In each sample, the molar fractions of the coordinated (*R*)- and (*S*)-enantiomers (*x* and *y*, respectively) are given by the following eqs 1 and could be straightforwardly determined if the chemical shifts of the two pure diastereomers (δ_R^{coord} and δ_S^{coord}) could be measured. Assuming rapid associative equilibria (eqs 2 and 3, where M represents the Ag−diamine fragment and *R* and *S* represent the two alkene enantiomers), and given the overall composition of each sample, the equilibrium constants could then be computed for each solution by a straightforward application of the mass action law and mass balances. However, the chemical shifts of the pure diastereomers could only be determined approximately in advance, because the complexes are weak and some dissociation takes place even when the diamine−metal fragment is in excess. Therefore the determination of the association constants of the two enantiomeric alkenes was carried out via an iterative least-squares procedure (run by a computer program specifically written for the problem), in which the chemical shifts of the pure diastereomers (δ_R^{coord} and δ_S^{coord}) were also optimized through the fitting. The equilibrium constants determined by the above method

Table 5. Association and Diastereoselectivity Equilibrium Constants for Complexes 8B and 8C[a]

complex-counterion	solvent	$10^{-3}\,K_R$	$10^{-3}\,K_S$	$K_{sel} = K_R/K_S$
8B-OTf	$CDCl_3$	21 ± 3	8.9 ± 0.9	2.70 ± 0.05
8B-NO_3	CD_2Cl_2	2.0 ± 0.2	0.68 ± 0.09	2.9 ± 0.2
8B-BF_4	acetone-d_6	0.66 ± 0.12	0.22 ± 0.05	3.1 ± 0.1
8C-OTf	$CDCl_3$	2.4 ± 0.2	0.9 ± 0.1	2.66 ± 0.03

[a] The given equilibrium constants (and corresponding standard deviations) result from the average of the values obtained from the fittings based on the NMR signals from different protons and at two different concentration (in the range 10−40 mM).

are reported in Table 5, and an example of the agreement resulting from the fitting is given in Figure 11.

$$x = \frac{\delta_{RS}^{free} - \delta_R^{obs}}{\delta_{RS}^{free} - \delta_R^{coord}}$$

$$y = \frac{\delta_{RS}^{free} - \delta_S^{obs}}{\delta_{RS}^{free} - \delta_S^{coord}} \qquad (1)$$

As expected from previous preparative work,[9] the

$$M + R \rightleftharpoons MR \qquad K_R = ([MR]/[M][R]) \qquad (2)$$

$$M + S \rightleftharpoons MS \qquad K_S = ([MS]/[M][S]) \qquad (3)$$

complexes were found to be rather weak, their association constants being strongly affected by the coordinating ability of the solvent and counterion (Table 5). Nevertheless, the diastereoselectivity constants were much less sensitive, giving remarkably consistent values under the different conditions and displaying only a slight tendency to increase with increasing polarity of the solvent, in fair qualitative agreement with the computational results. It is worth noting that the selectivity for the coordination of the (*R*)-enantiomer is substantially lower than that determined[8] for the analogous Cu(I) complex (ca. 3 versus ca. 40). This difference is probably related to the larger size of the metal ion, which is expected to make the chiral pocket hosting the alkene ligand less "deep", thus reducing the steric contacts responsible for the enantiodiscrimination.

Complex 8C. For this complex, no low-temperature NMR experiments were performed. The enantioselectivity of the $[(N-N)Ag]^+$ fragment for the (*R*)-enantiomer of the chiral alkene was determined in $CDCl_3$ by the NMR titration method outlined above, starting from a solution of the complex [(N−N)Ag]OTf and measuring the ^1H NMR chemical shifts of the two enantiomers after the addition of increasing amounts of racemic alkene. The results are reported in Table 5 together with those obtained for the butenol complex **8B**. As qualitatively anticipated by the previous preparative work,[9] the association constant for the hydrocarbon alkene complex **8C** is about 10 times weaker than for the alkenol complex **8B**, although the selectivity for the coordination of the (*R*)-enantiomer turns out to be about the same.

Summary and Conclusions

The diastereomeric preferences for coordination of chiral alkenes to chiral silver−ethanediamine complexes in solution have been studied both experimentally and computationally. The final computational results agree well with the experimental measurements, especially in the case of a chiral alkene not bearing a polar substituent. In the case of a chiral alkene having a polar hydrogen-bonding hydroxy substituent proximal to the metal binding site, a good correlation between experimental and computational results is obtained only when the effect of the solvent has been approximated by the use of a continuum solvation model. Furthermore, the analysis depends strongly on the substitution pattern of the ligand. When this pattern sufficiently limits the conformational flexibility of the complexes, a stepwise exclusion of unfavorable portions of conformational space is allowed, and a good correlation between experimental and computational results is readily accomplished.

A goal of our further work is to develop computational methods for the design of new chiral ligands and metal complexes that will permit improved NMR determination of enantiomeric composition and preparative separation of chiral alkenes. A computational pre-screening of potential ligands would require substantially more rapid methods than the ones employed herein. To this end, an empirical force field model is currently being developed and will be reported in due course. With respect to developing practical preparative separations, we note that the selectivity obtained in precipitation experiments[9] is substantially higher than the selectivity in solution and that a predictive method that includes crystallization preference would require periodic boundary calculations, preferably with methods several orders of magnitude faster than the QM techniques employed herein.

Experimental Section

General Procedures. Reagents and solvents were reagent-grade and were used without further purification. The diamine **8** was prepared from the commercially available (1*S*,2*S*)-1,2-diphenyl-1,2-ethanediamine using a described procedure.[20] NMR spectra were recorded on a Bruker DRX-400 spectrometer.

Preparation of [Ag((*S*,*S*)-8)(CH_2=CH_2)]BF_4 (8A-BF_4). The complex was prepared by mixing stoichiometric amounts of the diamine **8** (122 mg, 0.255 mmol) and anhydrous silver fluoroborate (49 mg, 0.25 mmol) in CH_2Cl_2 (2 mL) saturated with ethylene. Addition of pentane under a stream of ethylene gave the compound as a colorless crystalline precipitate (155 mg, 0.22 mmol, 88% yield). ^1H NMR (400 MHz, CD_2Cl_2): δ 2.25 (app s, 18H, Me), 3.33 (m, 2H, NH), 3.48 (m, 2H, NC*H*H), 3.57 (m, 2H, NCH*H*), 4.21 (s, 4H, CH_2=CH_2), 4.33 (m, 2H, NCH), 6.82 (s, 4H, Ar), 7.2−7.4 (m, 10H, Ph). ^{13}C NMR (100.6 MHz, CD_2Cl_2): δ 20.0 (*o*-Me), 21.0 (*p*-Me), 46.5 (NCH_2), 68.8 (NCH), 103.2 (CH_2=CH_2), 128.3, 129.0, 129.6, 133.4, 137.4, 138.2, 139.1 (aromatic C).

Preparation of [Ag((*S*,*S*)-8)((*R*)-CH_2=CHCH(OH)Me)]-BF_4 (8B-BF_4). Stoichiometric amounts of the diamine **8** (245 mg, 0.51 mmol) and anhydrous silver fluoroborate (98 mg, 0.50 mmol) were added to a solution of racemic 1-buten,3-ol (180 mg, 2.5 mmol) in CH_2Cl_2 (5 mL) containing a few drops of

(20) Corey, E. G.; DaSilva Jardine, P.; Virgil, S.; Yuen, P. W.; Connell, R. D. *J. Am. Chem. Soc.* **1989**, *111*, 9243−9244

acetone. Diethyl ether (5 mL) was added dropwise to the solution, and the mixture was kept in a freezer for 2 h, resulting in the crystallization of the complex as colorless needles (290 mg, 78% yield, 70% ee based on ^{1}H NMR). The analytical sample was obtained by slow crystallization from CH_2Cl_2/acetone and contained 1 mol of acetone/mol Ag. Anal. Calcd for $C_{41}H_{54}AgBF_4N_2O_2$: C, 61.44; H, 6.79; N, 3.49. Found: C, 61.13; H, 6.90; N, 3.28. ^{1}H NMR (400 MHz, CD_2Cl_2): δ 0.82 (d, 3H, Me), 2.25 (app s, 18H, ArMe), 2.90 (d, 1H, OH), 3.10 (m, 1H, C*H*OH), 3.16 (m, 2H, NH), 3.47 (m, 2H, NC*H*H), 3.63 (m, 2H, NCH*H*), 3.84 (d, 1H, =CH^{1Z}), 4.33 (m, 2H, CHPh), 4.35 (d, 1H, =CH^{1E}), 5.12 (ddd, 1H, =CH^2), 6.81 (s, 4H, Ar), 7.15−7.4 (m, 10H, Ph). The minor diastereomer (ca. 15% abundance), containing the (*S*)-butenol, gives separate signals for the coordinated allylic alcohol (but *not* for the diamine ligand): δ 1.90 (br, OH), 3.55 (m, C*H*OH), 3.93 (d, =CH^{1E}), 4.11 (d, =CH^{1Z}), 5.03 (ddd, =CH^2). ^{13}C NMR (100.6 MHz, CD_2Cl_2): δ 20.1 (*o*-Me (N−N)), 21.0 (*p*-Me (N−N)), 23.8 (Me), 46.7 (NCH_2), 66,6 (CHOH), 68.8 (NCH), 88.4 (=CH_2), 131.9 (=CH), 128.2, 129.0, 129.2, 133.2, 137.8, 138.2, 139.2 (aromatic C).

[Ag((*S,S*)-8)((*R*)-CH_2=CHCHCMe$_3$)]OTf (8C). This compound was not isolated. For the ^{1}H NMR determination of the enantioselectivity equilibrium constants (see below), the complex was generated in situ. Characterization data of the corresponding nitrate salt have been reported previously.[9]

Determination of the Binding Constants of the Enantiomeric Olefins to the Fragment [Ag((*S,S*)-8)]X (X = OTf, NO_3, BF_4). To an NMR tube containing a known amount of the silver−diamine complex (prepared separately in the case of the triflate and nitrate salts,[9] generated in situ in the case of the fluoroborate salt) dissolved in 0.750 mL of the appropriate deuterated solvent were added progressive measured amounts of the racemic olefin from a 10.0% (v/v) stock solution in the same solvent, and the ^{1}H NMR shifts of the enantiomeric olefins were carefully measured after each addition (see Tables S1a−S4a in Supporting Information as an example). The measurements were repeated at two different complex concentrations (in the range 10−50 mM) and covered a range of racemic olefin/metal ratio from 0.5 to 5. The values of the binding constants were optimized along with the chemical shifts of the "pure" complexes (see text), using the chemical shift data of each proton separately (see Tables S1b−S4b in Supporting Information for an example) and then averaged to produce the final results.

Acknowledgment. We are grateful for the award of a J. Peter Grace Prize Fellowship and a Reilly Fellowship to E.K., for financial support from the University of Notre Dame, Procter & Gamble Pharmaceuticals, and the MIUR (PRIN Grant No. 2002-031332), and for access to the NMR facilities of the CIMCF, Università di Napoli Federico II.

Supporting Information Available: Cartesian coordinates, zero-point-corrected energies, and lowest frequencies of the main complexes. Variable temperature 1H NMR spectra (Figures S1−S4). Examples of titration experiments (Tables S1−S4). This material is available free of charge via the Internet at http://pubs.acs.org.

OM050275T